Am J Transl Res 2022;14(12):8640-8649
www.ajtr.org /ISSN:1943-8141/AJTR0147316

Original Article

Radiomics analysis of unaffected side changes in classic trigeminal neuralgia

Lei Pan[1], Haiqi Ye[1], Xiaofen Zhu[1], Luoyu Wang[2], Xiuhong Ge[1]

[1]*Department of Radiology, Affiliated Hangzhou First People's Hospital, Zhejiang University School of Medicine, Hangzhou 310000, Zhejiang, China;* [2]*Laboratory of Oncology Research Diagnosis and Treatment, Affiliated Hangzhou First People's Hospital, Zhejiang University School of Medicine, Hangzhou 310000, Zhejiang, China*

Received October 27, 2022; Accepted November 16, 2022; Epub December 15, 2022; Published December 30, 2022

Abstract: Objective: To investigate the subtle differences in the structure of the unaffected trigeminal nerve between patients with classic trigeminal neuralgia (CTN) and healthy controls (HCs) by means of radiomics, so as to further explore the etiological mechanism of trigeminal neuralgia (TN). Methods: The imagine data of 95 CTN patients and 89 matched HCs were collected and retrospectively analyzed. They were assigned to four groups according to the presence or absence of neurovascular compression (NVC) of the unaffected trigeminal nerve (HCs with and without NVC; CTN patients with and without NVC on the unaffected side). All patients underwent magnetic resonance imaging (MRI) scans. Bilateral trigeminal cisternal segments were manually delineated, followed by feature extraction, dimensionality reduction, feature selection, model construction and model evaluation. Results: Six weighted textural signatures (sphericity, maximum 2D diameter, skewness, robust mean absolute deviation, large dependence low gray level emphasis, and surface-to-volume ratio) were found in HCs with and without NVC, while 7 were found in CTN patients without NVC on the unaffected side and HCs without NVC. The Rad_score was statistically different between the two groups ($P < 0.05$). The AUC of the training set was consistent with that of the validation set. The calibration curves of the training and validation sets demonstrated the high accuracy of the model. Conclusions: NVC can alter trigeminal nerve structure and cause alterations in related characteristics; but NVC is not a necessary condition for the formation of CTN, and its incidence is also high in asymptomatic healthy people, and thus it is necessary to grade the severity of NVC. In addition, there are differences in the characteristics of the unaffected side between CTN patients and HCs, which may be due to congenital or secondary factors.

Keywords: Radiomics, classic trigeminal neuralgia, neurovascular compression, unaffected side

Introduction

Trigeminal neuralgia (TN) is a debilitating chronic facial pain disease that is typically characterized by extremely intense, sporadic and shock-like unilateral pain episodes [1]. The sensory information of the craniofacial region is transmitted by the trigeminal sensory system, which is composed of peripheral structures (trigeminal nerve, trigeminal ganglion, etc.) and central structures (e.g., trigeminal brainstem sensory nuclear complex) [2]. It can be either triggered by stimulation of trigeminal sensitive areas or occur spontaneously. The incidence rate is estimated to be 4 to 13 per 100000 people per year. The pain is often described as tingling, paroxysmal, reminiscent of electric shock or burning, and is limited to areas dominated by one or more branches of the trigeminal nerve [3]. The etiology of TN and the underlying mechanisms of this condition are still poorly understood; but based on the etiology, it is mainly categorized as primary TN (or classic TN, CTN), secondary TN or idiopathic TN [4-6].

Neurovascular compression (NVC) is considered to be the main cause of CTN, which can be treated by microvascular decompression (MVD) [7, 8]. Preoperative high-resolution 3D magnetic resonance imaging (MRI) has been shown to be a reliable tool to diagnose NVC in CTN patients. However, the NVC theory has been controversial from the very beginning. The NVC hypothesis is based on the fact that most patients achieved sustained pain after microvascular decompression surgery relief. Despite this evidence, NVC can also be observed in asymptomatic patients [9, 10]. This anatomical

variation is also present in 25-49% of healthy individuals and 14-39% of cadavers [11]. Studies on the incidence, extent, and characteristics of NVC in asymptomatic individuals remain scarce. Neuroimaging studies have shown altered brain structure, function and connectivity of TN patients that have been confirmed by different methods [12-15]. Here, we invetigate the subtle differences in the structure of the unaffected trigeminal nerve from the intra-group comparison among healthy controls (HCs) and the inter-group comparison between CTN patients and HCs, and to explore the possible etiological mechanism of TN from multiple perspectives.

Materials and methods

Research participants

This study was conducted after obtaining approval from the Ethics Committee of Affiliated Hangzhou First People's Hospital Zhejiang University School of Medicine (IRB# No. 202107002). From July 2021 to December 2021, the clinical and imaging data of CTN patients who visited the Affiliated Hangzhou First People's Hospital Zhejiang University School of Medicine and underwent MRI scanning were collected for retrospective analysis. Patients' inclusion criteria: (1) Conforming to the diagnostic criteria of the International Classification of Headache Disorders, 3rd edition (ICHD-3) for CTN [8]; (2) Patients with unilateral symptoms; (3) Those who underwent a complete MRI scan, such as volume interpolated breath-hold examination (3D-VIBE) and 3D short tau inversion recovery (3D-STIR) sequence; (4) Patients with dextromanuality. Exclusion criteria: (1) Patients with previous TN-related surgery; (2) Patients with clear history of neurological diseases such as brain trauma, cerebral hemorrhage or brain tumors; (3) Patients with image artifacts or poor quality that affect the final evaluation. Finally, 95 patients were retrospectively enrolled and grouped as follows according to the presence or absence of NVC of the unaffected trigeminal nerve: CTN patients with NVC on the unaffected side and CTN patients without NVC on the unaffected side.

Additionally, sex- and age-matching HCs were included. Inclusion criteria for HCs: (1) No history of neurological, psychiatric or pain diseases; (2) No history of major central nervous system surgery; (3) No contraindications to MRI scanning. Exclusion criteria: (1) Previous TN-related surgery; (2) Those did not undergo a complete MRI scan; (3) Image artifacts or poor quality that affect the final evaluation. After screening, 89 HCs were included, and similarly, they were assigned to HCs with NVC and HCs without NVC according to the presence of NVC manifestations of the trigeminal nerve.

Three experienced diagnosticians judged and evaluated the presence and extent of NVC based on preoperative MRI. The extent of NVC was divided into contact only, compression (indentation on nerve surface) and deformity (nerve deviation or distortion) [16].

Inspection methods

All brain scans were performed with a 3.0T MRI scanner (Discovery MR Verio, Siemens, Germany) and an 8 channel phased-array head coil, with participants placed in the supine position. Foam pads and headphones were used to reduce head movement and scanner noise. The following two sets of sequences were used to scan and capture images.

(1) 3D-VIBE sequence: repetition time 10 ms, echo time 3.69 ms, flip angle 12°, field of view 220×220, voxel 0.8×0.8×0.8, layer thickness 0.8 mm, 60 axial slices.

(2) 3D-STIR sequence: repetition time 3800 ms, echo time 194 ms, flip angle 12°, field of view 230×230, voxel 0.9×0.9×0.9, layer thickness 0.9 mm, 64 axial slices.

Radiomics and machine learning analysis

The imaging features of bilateral trigeminal nerves of the subjects were analyzed using the uAI Research Portal (United Imaging Intelligence) software. The specific steps were as follows: ① Determination of regions of interest (ROIs): the trigeminal cistern segment was manually delineated layer by layer on the images of 3D-VIBE sequence (from the position where the nerve left the pons to the entrance of the Meckel's cavity), avoiding the responsible vessels; ② Feature extraction: based on the original image and ROIs, the following features were extracted from feature categories: first order, shape, gray-level co-occurrence matrix (GLCM), gray-level size zone matrix (GLSZM),

gray-level run-length matrix (GLRLM), neighborhood gray-tone difference matrix (NGTDM) and gray-level dependence matrix (GLDM); ③ Feature selection: two feature selection methods, namely, minimum redundancy maximum relevance (mRMR), and least absolute shrinkage and selection operator regression (LASSO), were used for dimensionality reduction. mRMR was used first to eliminate redundant and irrelevant features, after which LASSO was utilized to select the most predictive feature subsets and evaluate the corresponding coefficients; ④ Model construction: the ratios of the training set and the validation set were randomly set to 0.7 and 0.3, respectively. A radiomics signature (Rad-score) was calculated for each patient via a linear combination of selected features that were weighted by their respective coefficients and compared between the training and validation sets. Radiologic scores were then combined with independent clinicoradiological predictors to construct a comprehensive logistic regression-based nomogram; ⑤ Model evaluation: first, the differences were quantified by the area under the receiver operating characteristic (ROC) curve (AUC), and then the calibration curve was applied to estimate the consistency between the prediction model and the actual results. Finally, the clinical net benefit of the prediction model was visualized by the decision curve. See **Figure 1** for details.

Statistics and methods

Statistical analyses were performed using SPSS 26.0 and R language (V.3.6.1). Categorical data were presented as the number of cases (percentage) while measurement data conforming to a normal distribution was presented as mean ± standard deviation. Clinical and MRI morphological features were assessed using the Chi-square test (nominal variables) and Wilcoxon test (continuous variables). The model effectiveness was evaluated by analyzing the ROC curve of the machine learning module to obtain the AUC and other model evaluation indexes. *P* value < 0.05 indicated the presence of statistical significance.

Results

Clinical data

Clinical grouping and clinical data comparison between groups: According to the presence or absence of NVC manifestations of the unaffected trigeminal nerve, the subjects were divided into four groups: CTN patients with NVC on the unaffected side, CTN patients without NVC on the unaffected side, HCs with NVC, and HCs without NVC. No significant differences were found in number, sex and age between CTN patients and HCs ($P > 0.05$). See **Table 1** for details.

Statistics of clinical data of HCs with NVC: The data showed that 62.9% (56/89) of HCs had NVC manifestations; the probability of developing bilateral NVC was 30.3% (27/89), and the incidence of NVC in all nerves was 46.6% (83/178); the possibility of NVC occurring on the left side, which accounted for 56.6% (47/83), was slightly higher than that on the right side. Females were found to be slightly more susceptible to NVC than males, accounting for 58.9% (33/56). Of all nerves in HCs with NVC, the overwhelming majority (96.4%) of NVC showed only contact or indentation without significant nerve deformity or deviation; only three nerves had grade 3 compression that occurred in the right mid-distal segment, two of which were obviously compressed by the vertebrobasilar artery, and the third was compressed by the superior cerebellar artery to form an obvious indentation. The most common offending vessel was the superior cerebellar artery (89.2%), and the most common compression site was the mid-distal part of the cistern segment (62.7%). No significant atrophic manifestations were observed when comparing NVC with uncompressed nerve cross-section and cross-sectional area. See **Table 2** for details.

Radiomics analysis

HCs with and without NVC: A total of 117 features were selected from each ROI. After dimensionality reduction using mRMR and LASSO, 6 weighted textural signatures were selected, including sphericity, maximum 2D diameter (column), skewness, robust mean absolute deviation (rMAD), large dependence low gray level emphasis (LDLGLE) and surface-to-volume ratio (S/V). The Rad_score was statistically different between HCs with and without NVC ($P < 0.05$). Details are shown in **Figure 2**.

CTN patients without NVC on the unaffected side and HCs without NVC: A total of 117 signatures were extracted from each ROI. After

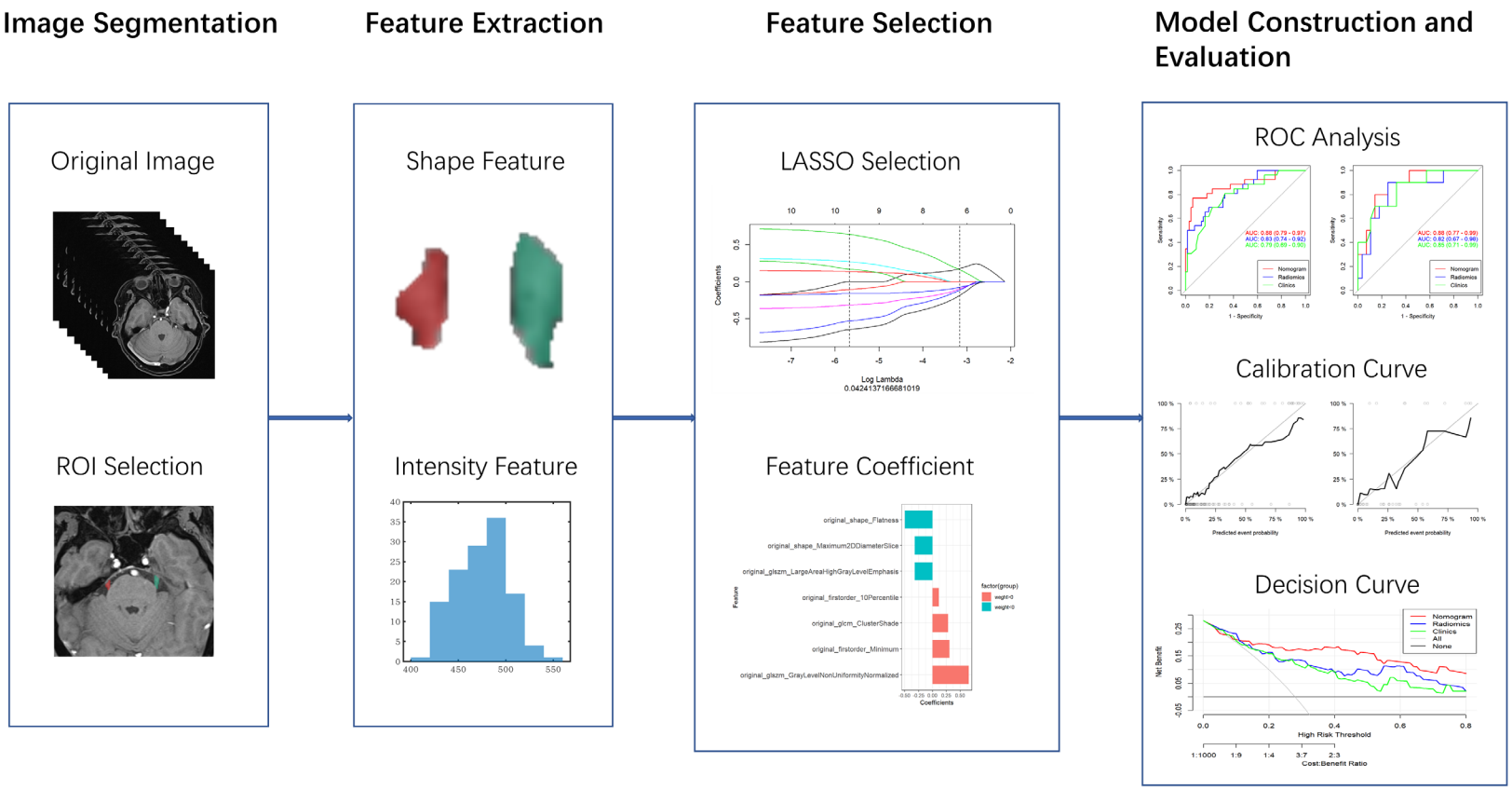

Figure 1. Flow chart of radiomics analysis. ROI, regions of interest; LASSO, least absolute shrinkage and selection operator; ROC, receiver operating characteristic curve.

Table 1. Clinical data of CTN patients and healthy controls

		CTN patients (on the unaffected side, n=95)	Healthy controls (n=89)	χ^2/t	P
Number	NVC_1	59 (62.1)	56 (62.9)	0.013	0.909[a]
	NVC_0	36 (37.9)	33 (37.1)		
Sex (M/F)	NVC_1	22/37	23/33	0.173	0.678[a]
	NVC_0	15/21	10/23	0.962	0.327[a]
Age	NVC_1	53.1±11.9	52.2±12.3	0.399	0.692[b]
	NVC_0	52.9±12.2	51.6±11.8	0.449	0.650[b]

CTN, classical trigeminal neuralgia; NVC, neurovascular compression; NVC_1, with NVC; NVC_0, without NVC; P[a], Chi-square test; P[b], independent-sample t test.

Table 2. Clinical data of healthy controls with NVC

	Left side	Right side	Total	χ^2	P
Ofv				3.338	0.342
Superior cerebellar artery	43 (58.1)	31 (41.9)	74		
Anterior superior cerebellar artery	1 (33.3)	2 (66.7)	3		
Anterior inferior cerebellar artery	0 (0)	1 (100.0)	1		
Vertebral artery/basilar artery	0 (0)	2 (100.0)	2		
Arteriole	3 (100.0)	0 (0)	3		
POfvC				0.506	0.477
Proximal 1/3	16 (51.6)	15 (48.4)	31		
Mid-distal 2/3	31 (59.6)	21 (40.4)	52		
DOfvC				4.809	0.090
Contact only	21 (53.8)	18 (46.2)	39		
Indentation	26 (63.4)	15 (36.6)	41		
Deviation and deformity	0 (0)	3 (100.0)	3		

Ofv, offending vessel; POfvC, the position of offending vascular compression; DOfvC, the degree of offending vascular compression.

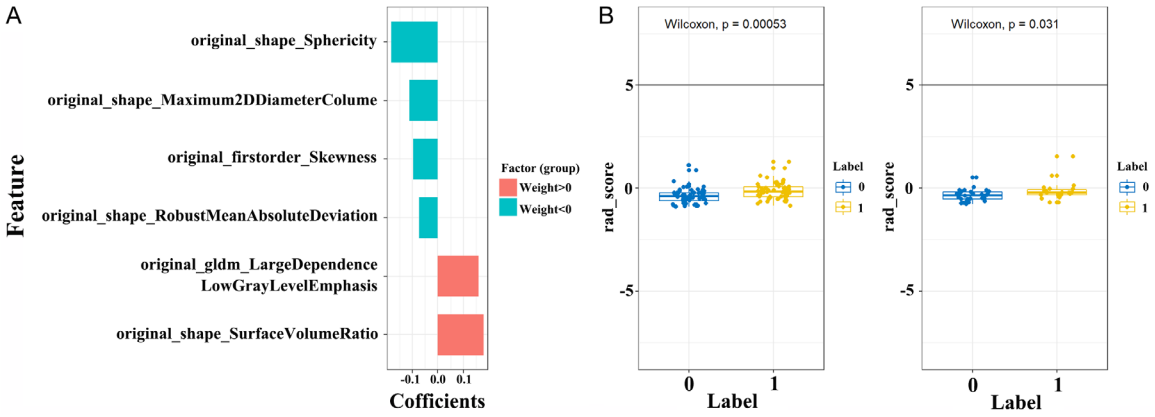

Figure 2. Feature selection of HCs with and without NVC. A. Wilcoxon's test of the Rad score between the two groups of trigeminal-nerve cisternal segment feature selection and importance ratio. B. Wilcoxon's test of Rad score in the training set and the validation set. HCs, healthy controls; NVC, neurovascular compression; 0, without NVC; 1, with NVC.

dimensionality reduction by mRMR and LASSO, seven weighted textural signatures were selected, including flatness, maximum 2D diameter (slice), large area high gray level emphasis (LAHGLE), 10th percentile, cluster shade, minimum, and gray level non-uniformity normalized

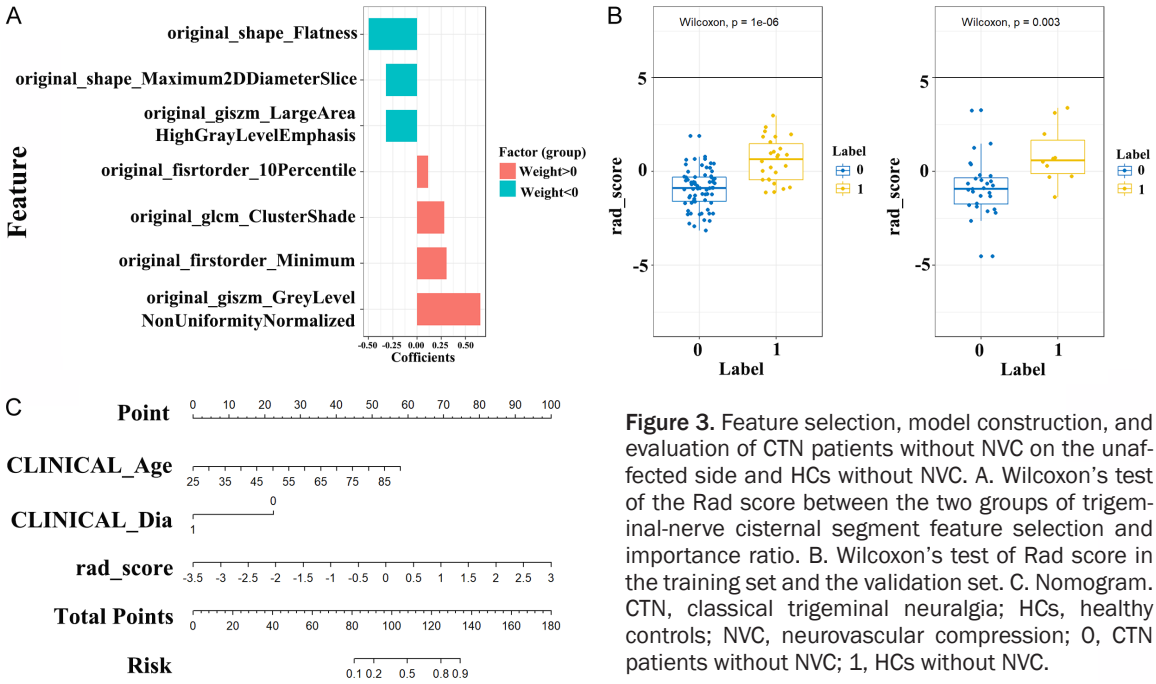

Figure 3. Feature selection, model construction, and evaluation of CTN patients without NVC on the unaffected side and HCs without NVC. A. Wilcoxon's test of the Rad score between the two groups of trigeminal-nerve cisternal segment feature selection and importance ratio. B. Wilcoxon's test of Rad score in the training set and the validation set. C. Nomogram. CTN, classical trigeminal neuralgia; HCs, healthy controls; NVC, neurovascular compression; 0, CTN patients without NVC; 1, HCs without NVC.

(GLNN). The Rad_score differed statistically between CTN patients without NVC on the unaffected side and HCs without NVC ($P < 0.05$). The AUC of the training set was consistent with that of the validation set, demonstrating good fit of the model. A nomogram was constructed, which visually simplified the complex regression equation. The calibration curves of the training set and validation set demonstrated the high accuracy of the model. Finally, the clinical practicability of the model was assessed using a decision curve. Details are shown in **Figures 3** and **4**.

Discussion

TN, a complex oral and facial pain syndrome, is characterized by unilateral paroxysmal stabbing pain in the trigeminal nerve distribution area. The specific pathogenesis is still unclear. Patients with TN often feel nervous or fearful of pain as it may come at any time. This has severely impacted on patients' daily life, such as talking, eating, tooth brushing, face washing, and even the most basic social activities. Under such huge pressure for a long time, they are prone to anxiety and depression, leading to a continuous decline in their quality of life. Therefore, it is of great clinical significance to have a deeper understanding of its etiological mechanism, so as to treat patients more efficiently.

Clinically, NVC is widely supported as the main theoretical basis for the pathogenesis of CTN, in which demyelination along with the trigeminal afferent pathway is considered as the core element. These are basically consistent with our previous research findings and arguments [17]. Many brain structure studies found that changes in gray matter volume in CTN patients mainly involved primary in somatosensory cortex, insula, thalamus, anterior cingulate cortex, basal ganglia, hippocampus, temporal lobe cortex and cerebellum, with the most obvious changes in pain matrix [18-20]. At the same time, functional magnetic resonance imaging (fMRI) studies in CTN patients revealed brain dysfunction, mainly distributed in the prefrontal, temporal and parietal lobes, posterior cingulate cortex, insula and cerebellum, especially the prominent network and default mode network [21-23].

The first set of comparative data in this study was obtained from HCs with and without NVC. The results revealed six weighted textural signatures, namely, sphericity, maximum 2D diameter (column), skewness, rMAD, LDLGLE and S/V. The reason may be that NVC causes trigeminal nerve deviation, deformity or even demyelination after long-term compression, which in turn leads to changes in the above-mentioned characteristics. In recent years, some researchers recruited subjects with NVC

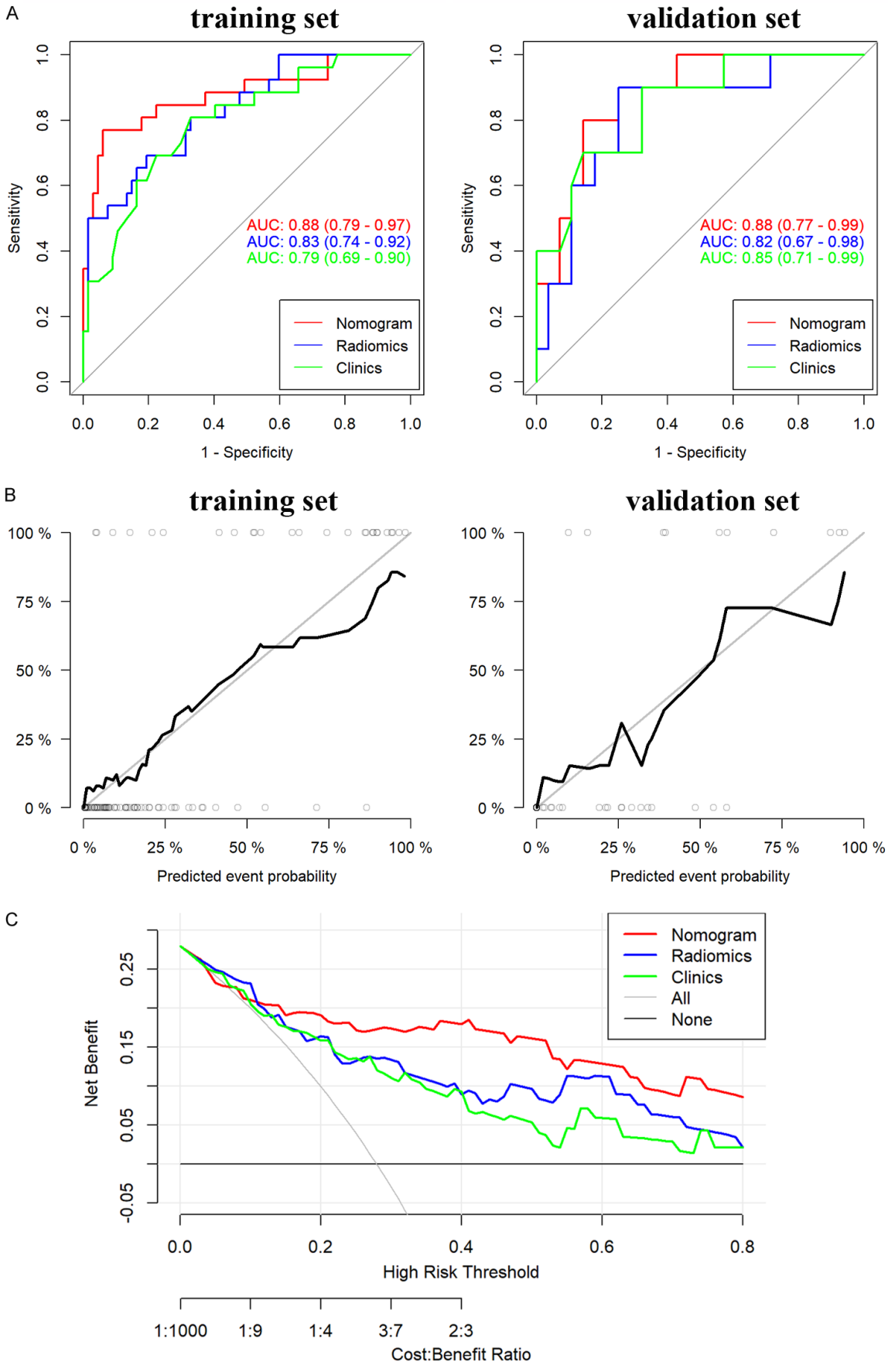
A
training set
validation set
Sensitivity
1 - Specificity
AUC: 0.88 (0.79 - 0.97)
AUC: 0.83 (0.74 - 0.92)
AUC: 0.79 (0.69 - 0.90)
AUC: 0.88 (0.77 - 0.99)
AUC: 0.82 (0.67 - 0.98)
AUC: 0.85 (0.71 - 0.99)
Nomogram
Radiomics
Clinics
B
training set
validation set
Predicted event probability
C
Net Benefit
High Risk Threshold
Cost:Benefit Ratio
1:1000
1:9
1:4
3:7
2:3
All
None

Figure 4. Validation of the three models in training and validation set. A. ROC of training set and validation set of the three models; B. Calibration curve of training set and validation set; C. Decision curve. ROC, receiver operating characteristic curve.

but no history of facial pain as a healthy control group, and used diffusion tensor imaging (DTI scans) to observe the functional changes caused by NVC [24]. The results showed no statistical difference in DTI parameters between the compressed side and the uncompressed side in the healthy control group, which was different from our findings. The reason may be that DTI scan results are diffusion correlation coefficients, while this study scanned the trigeminal nerve structure. In addition, the comparative data of HCs with and without NVC only selected textural signatures but did not perform model building. The is because for healthy people, the bilateral trigeminal nerves are all from the healthy sides, and the presence or absence of NVC can be identified by naked eyes, so the construction of the model does not have clinical significance.

Although HCs can also have NVC in the trigeminal nerve and the above-mentioned characteristics, they do not show the corresponding symptoms of CTN, which also indicates that the presence of NVC does not necessarily mean the occurrence of CTN. Anatomical studies demonstrated a high neurovascular contact rate between the trigeminal nerve and the cerebellopontine angle (CPA) blood vessels in subjects known to have no CTN. Panczykowski et al. [24] reported that the incidence of NVC in 22 TN patients was not significantly different from that of their matched controls, with similar distribution and location of compressed blood vessels. But their study did not analyze the compression degree of the trigeminal nerve. Maarbjerg et al. [25] reported that in 135 CTN patients screened with 3T MRI using 3D balanced fast field-echo sequences, NVC was found in 89% of symptomatic patients and 78% of asymptomatic patients; when only severe compression (that is, compression with nerve depression or atrophy) is considered, the incidence of NVC is different between the symptomatic side (53%) and the asymptomatic side (13%). Therefore, it is suggested that the MRI signs of particularly severe NVC should be regarded as surgical indications for MVD.

This study also used 3T MRI for scanning and used NVC grading as one of the important parameters (see **Table 2** for details). The results showed that the contact between trigeminal nerve and posterior cranial fossa vessels was indeed frequent in asymptomatic subjects, but most of the compression was too mild to show corresponding clinical symptoms. In contrast, NVC of typical TN usually presents with moderate or severe compression, with root entry zone (REZ) being the major compression site [26]. Therefore, mere contact between blood vessels and the trigeminal nerve demonstrated by high-resolution 3T MRI scans should be considered an anatomical variant with no pathological significance; conversely, severe compression of the trigeminal nerve in patients with facial pain must be considered as a clear etiology, in which case MVD surgery is recommended. In addition, older age may lead to elongation and tortuosity of the vertebrobasilar artery system and its branches, thereby increasing the risk of neurovascular contact in the posterior fossa, where progressive artery elongation due to age and hypertension increases the degree of compression, a hypothesis supported by the higher incidence of TN in the elderly [27].

The second set of comparative data in this study was derived from CTN patients without NVC on the unaffected side and HCs without NVC. The seven weighted textural signatures determined were flatness, maximum 2D diameter (slice), LAHGLE, 10th percentile, cluster shade, minimum, and GLNN, which indicates that although the unaffected CTN can be equally NVC-free and asymptomatic, there are still many characteristic differences between it and the healthy control group. In this regard, we mainly hold the following two views: first, there may be congenital differences in trigeminal nerve structure in CTN patients, such as genetic factors. For example, Gambeta et al. [28] found that the P2455H variant in the CACNA1A gene can cause the enhancement or deletion of Cav2.1 function, which may affect signal processing of the trigeminal nervous system. Another possibility is that CTN causes secondary changes in the trigeminal nerve structure, such as compensatory thickening of the unaffected side due to atrophy of the affected side, which is worth of investigation in subsequent studies. Furthermore, although model construction and evaluation have been carried out for the comparison of this dataset, the main

purpose is not to diagnose the disease or predict curative effects, but to provide more scientific basis for data, so as to better verify the differences between the two datasets.

In this study, we directly delineated the cisterna segment of the trigeminal nerve and analyzes the textural signatures through radiomics; moreover, it is a prospective study, while the current CTN radiomics studies at home and abroad are mostly based on whole-brain analysis. However, this is a single-center cross-sectional study with a small sample size. In the future, it can be expanded into a multi-center study, so that the data and conclusions can be more convincing. Besides, a longitudinal study in combination with the data after MVD can be added to perform classification modeling and efficacy prediction evaluation of patients.

Conclusion

CTN has traditionally been diagnosed by clinicians based on the patient's symptoms. The rapid development of MRI technology and artificial intelligence in recent years has provided us with more ways to understand the morphological anatomy of CTN, which helps clinicians to understand the pathogenesis of CTN from multiple dimensions, and to better carry out and guide treatment.

Acknowledgements

National Natural Science Foundation of China (81871337), Zhejiang Provincial Public Welfare Research Project (2021RC108, 2020RC092), Medical and Health Technology Project of Hangzhou (A20200507), Hangzhou Agriculture and Social Development Scientific Research Guidance Project (20211231Y022).

Disclosure of conflict of interest

None.

Address correspondence to: Xiuhong Ge, Department of Radiology, Affiliated Hangzhou First People's Hospital, Zhejiang University School of Medicine, Hangzhou 310000, Zhejiang, China. Tel: +86-15068858093; E-mail: zjhzsy003@126.com

References

[1] Tohyama S, Walker MR, Zhang JY, Cheng JC and Hodaie M. Brainstem trigeminal fiber microstructural abnormalities are associated with treatment response across subtypes of trigeminal neuralgia. Pain 2021; 162: 1790-1799.

[2] Sessle B. Mechanisms of oral somatosensory and motor functions and their clinical correlates. J Oral Rehabil 2006; 33: 243-261.

[3] Gambeta E, Chichorro JG and Zamponi GW. Trigeminal neuralgia: an overview from pathophysiology to pharmacological treatments. Mol Pain 2020; 16: 1744806920901890.

[4] Jones MR, Urits I, Ehrhardt KP, Cefalu JN, Kendrick JB, Park DJ, Cornett EM, Kaye AD and Viswanath O. A comprehensive review of trigeminal neuralgia. Curr Pain Headache Rep 2019; 23: 74.

[5] Cruccu G, Di Stefano G and Truini A. Trigeminal neuralgia. N Engl J Med 2020; 383: 754-762.

[6] Leal PR, Hermier M, Froment JC, Souza MA, Cristino-Filho G and Sindou M. Preoperative demonstration of the neurovascular compression characteristics with special emphasis on the degree of compression, using high-resolution magnetic resonance imaging: a prospective study, with comparison to surgical findings, in 100 consecutive patients who underwent microvascular decompression for trigeminal neuralgia. Acta Neurochir (Wien) 2010; 152: 817-825.

[7] Cruccu G. Trigeminal neuralgia. Continuum (Minneap Minn) 2017; 23: 396-420.

[8] Arnold M. Headache classification committee of the international headache society (IHS) the international classification of headache disorders. Cephalalgia 2018; 38: 1-211.

[9] Zakrzewska JM and Akram H. Neurosurgical interventions for the treatment of classical trigeminal neuralgia. Cochrane Database Syst Rev 2011; 2011: CD007312.

[10] Ferguson G, Brett D, Peerless S, Barr H and Girvin J. Trigeminal neuralgia: a comparison of the results of percutaneous rhizotomy and microvascular decompression. Can J Neurol Sci 1981; 8: 207-214.

[11] Wang Y, Yang Q, Cao D, Seminowicz D, Remeniuk B, Gao L and Zhang M. Correlation between nerve atrophy, brain grey matter volume and pain severity in patients with primary trigeminal neuralgia. Cephalalgia 2019; 39: 515-525.

[12] Wang Y, Cao DY, Remeniuk B, Krimmel S, Seminowicz DA and Zhang M. Altered brain structure and function associated with sensory and affective components of classic trigeminal neuralgia. Pain 2017; 158: 1561-1570.

[13] Wang Y, Xu C, Zhai L, Lu X, Wu X, Yi Y, Liu Z, Guan Q and Zhang X. Spatial-temporal signature of resting-state BOLD signals in classic trigeminal neuralgia. J Pain Res 2017; 10: 2741-2750.

[14] Zhang Y, Mao Z, Pan L, Ling Z, Liu X, Zhang J and Yu X. Frequency-specific alterations in cortical rhythms and functional connectivity in trigeminal neuralgia. Brain Imaging Behav 2019; 13: 1497-1509.
[15] Ge X, Wang L, Pan L, Ye H, Zhu X, Feng Q and Ding Z. Risk factors for unilateral trigeminal neuralgia based on machine learning. Front Neurol 2022; 13: 862973.
[16] Jani RH, Hughes MA, Gold MS, Branstetter BF, Ligus ZE and Sekula RF Jr. Trigeminal nerve compression without trigeminal neuralgia: intraoperative vs imaging evidence. Neurosurgery 2019; 84: 60-65.
[17] Chai W, You C, Zhang W, Peng W, Tan L, Guan Y and Chen K. Diffusion tensor imaging of microstructural alterations in the trigeminal nerve due to neurovascular contact/compression. Acta Neurochir (Wien) 2019; 161: 1407-1413.
[18] Tsai YH, Yuan R, Patel D, Chandrasekaran S, Weng HH, Yang JT, Lin CP and Biswal BB. Altered structure and functional connection in patients with classical trigeminal neuralgia. Hum Brain Mapp 2018; 39: 609-621.
[19] Tang Y, Wang M, Zheng T, Yuan F, Yang H, Han F and Chen G. Grey matter volume alterations in trigeminal neuralgia: a systematic review and meta-analysis of voxel-based morphometry studies. Prog Neuropsychopharmacol Biol Psychiatry 2020; 98: 109821.
[20] Wu M, Jiang X, Qiu J, Fu X and Niu C. Gray and white matter abnormalities in primary trigeminal neuralgia with and without neurovascular compression. J Headache Pain 2020; 21: 136.
[21] Tsai YH, Liang X, Yang JT and Hsu LM. Modular organization of brain resting state networks in patients with classical trigeminal neuralgia. Neuroimage Clin 2019; 24: 102027.
[22] Zhang P, Jiang Y, Liu G, Han J, Wang J, Ma L, Hu W and Zhang J. Altered brain functional network dynamics in classic trigeminal neuralgia: a resting-state functional magnetic resonance imaging study. J Headache Pain 2021; 22: 147.
[23] Chen Y, Xiang CQ, Liu WF, Jiang N, Zhu PW, Ye L, Li B, Lin Q, Min YL and Su T. Application of amplitude of low-frequency fluctuation to altered spontaneous neuronal activity in classical trigeminal neuralgia patients: a resting-state functional MRI study. Mol Med Rep 2019; 20: 1707-1715.
[24] Panczykowski DM, Frederickson AM, Hughes MA, Oskin JE, Stevens DR and Sekula RF Jr. A blinded, case-control trial assessing the value of steady state free precession magnetic resonance imaging in the diagnosis of trigeminal neuralgia. World Neurosurg 2016; 89: 427-433.
[25] Maarbjerg S, Wolfram F, Gozalov A, Olesen J and Bendtsen L. Significance of neurovascular contact in classical trigeminal neuralgia. Brain 2015; 138: 311-319.
[26] Bendtsen L, Zakrzewska JM, Abbott J, Braschinsky M, Di Stefano G, Donnet A, Eide PK, Leal PRL, Maarbjerg S, May A, Nurmikko T, Obermann M, Jensen TS and Cruccu G. European Academy of Neurology guideline on trigeminal neuralgia. Eur J Neurol 2019; 26: 831-849.
[27] Greve T, Tonn JC and Mehrkens JH. Microvascular decompression for trigeminal neuralgia in the elderly: efficacy and safety. J Neurol 2021; 268: 532-540.
[28] Gambeta E, Gandini MA, Souza IA, Ferron L and Zamponi GW. A CACNA1A variant associated with trigeminal neuralgia alters the gating of Cav2. 1 channels. Mol Brain 2021; 14: 4.